
GEOLOGICAL, PETROGRAPHICAL AND GEOCHEMICAL STUDIES ON ZABARAH METASEDIMENTS, SOUTH EASTERN DESERT, EGYPT

Ahmed M. El-Mezayen¹, Hatem M. El-Desoky¹, Moatasemllah M. El-Kholy²

1. Geology Department, Faculty of Science, Al-Azhar University, PO Box 11884, Nasr City, Cairo, Egypt.

2. Egyptian Mineral Resources Authority, Cairo, Egypt.

ABSTRACT

The present work discusses the geological, petrographical and geochemical features of the metasediments in Wadi Zabarah area. Detailed field studies revealed that this area comprises two main rock types of the metasediments: 1) psammitic and psammopelitic schists and 2) cataclastic rocks. The psammitic and psammopelitic schists are classified according to grade of metamorphism into: tremolite-actinolite schists, graphite schists, tourmaline-bearing schists, beryl-bearing schists, quartzitic schists and garnet-bearing schists. Cataclastic rocks comprise protomylonitic, blastomylonitic and ultramylonitic schists. The geochemical characters of these rocks revealed that they are comparable with the non-peralkaline, peraluminous, continental and/or oceanic island arc sandstones.

Key words: Psammitic schists, mylonites, Eastern Desert, Egypt.

INTRODUCTION

Gabal Zabara is located at southwest of Marsa Alam coastal City, South Eastern Desert, Egypt. Between latitude 24°43'00" to 24°47'00"N and longitude 34°40'00" to 34°44'00"E. It is including ophiolitic mélangé and associated metasediments into which granodiorites and different granites rocks have been intruded. All these rocks are traversed by dykes and quartz veins (Soliman, 1986).

The petrological and geochemical investigation of the famous Egyptian emerald deposits in the Eastern Desert of Egypt indicate that emerald had been crystallized as syn- to post-tectonics in a black wall zoning sequence found between apogranitic gneisses and ultramafics belonging to a volcano-sediments of tectonic mélangé (Grundmann and Morteani, 1993). Garnet-amphibolites from the studied area are characterized by the assemblage: garnet-amphibole-epidote-plagioclase-ilmenite-rutile (Surour, 1995). The mineralization associated with tectonically emplaced shield edges and related trends in North Africa and the Arabian shield, and distinguished that the satellite images of North Africa and Arabia show five major lineaments located within the southern half of

the Tethyan Sea.

All the precious stone bearing are enclosed within regions rocks had subjected to high tensional forces of different directions. These forced result in emplacing the precambrian serpentinites (Hakki and Errumman, 1996). They attempted to distinguished green beryl of different hues from the gem emerald on the basis of their trace elements contents. It is evident that Cr impurities (together with V and Ni) contribute to the green coloration of beryl, especially the dark bluish-green variety which contains up to 5143ppm Cr (Surour *et al.*, 2002). Beryl in the Eastern Desert of Egypt occurs in two modes: Type (A) in quartz veins and pegmatites at the contact between the ophiolitic metapyroxenite and G3 biotite and muscovite granites. Type (B) which occurs as disseminated and veins affiliated to the G3 granites (Takla *et al.*, 2004).

GEOLOGIC SETTING

Gabal Zabarah area lies in the southern part of Egypt in the extremely arid desert environment of the South Eastern Desert. Metasediments represent the oldest rock units exposed in Gabal Zabarah and composed mainly of schists and cataclastic rocks. The psammitic and psammopelitic schists are

classified according to their low to medium grade metamorphism into the followings: - actinolite schists, graphite schists, tourmaline-bearing schists, beryl-bearing schists, quartzitic schists and garnet-bearing schists. Cataclastic rocks comprise protomylonitic, blastomylonitic and ultramylonitic schists (Fig.1).

1. Psammitic and psammopelitic schists

Psammitic and psammopelitic schists result from regional metamorphism, dominated at Wadi Umm Lasaf and characterized by highly foliations (Fig.2a). These schists are folded showing various

minor and mesoscopic refolded folds (Fig.2b), dipping layers of schists, quartzite extending parallel to the foliation planes of schists. Granitic rocks intruded the schists (Fig.2c). Quartz veins invading these schists or forming lenses within schists are recorded by intrusive contact.

In general, the schists are fine- to coarse-grained, varicolored from yellow to brown and varying from grey to dark grey. Schists and cataclastic rocks are the most dominant rock units especially at Wadi Umm-Lasaf, and have low distribution at Wadi El-Zarqa.

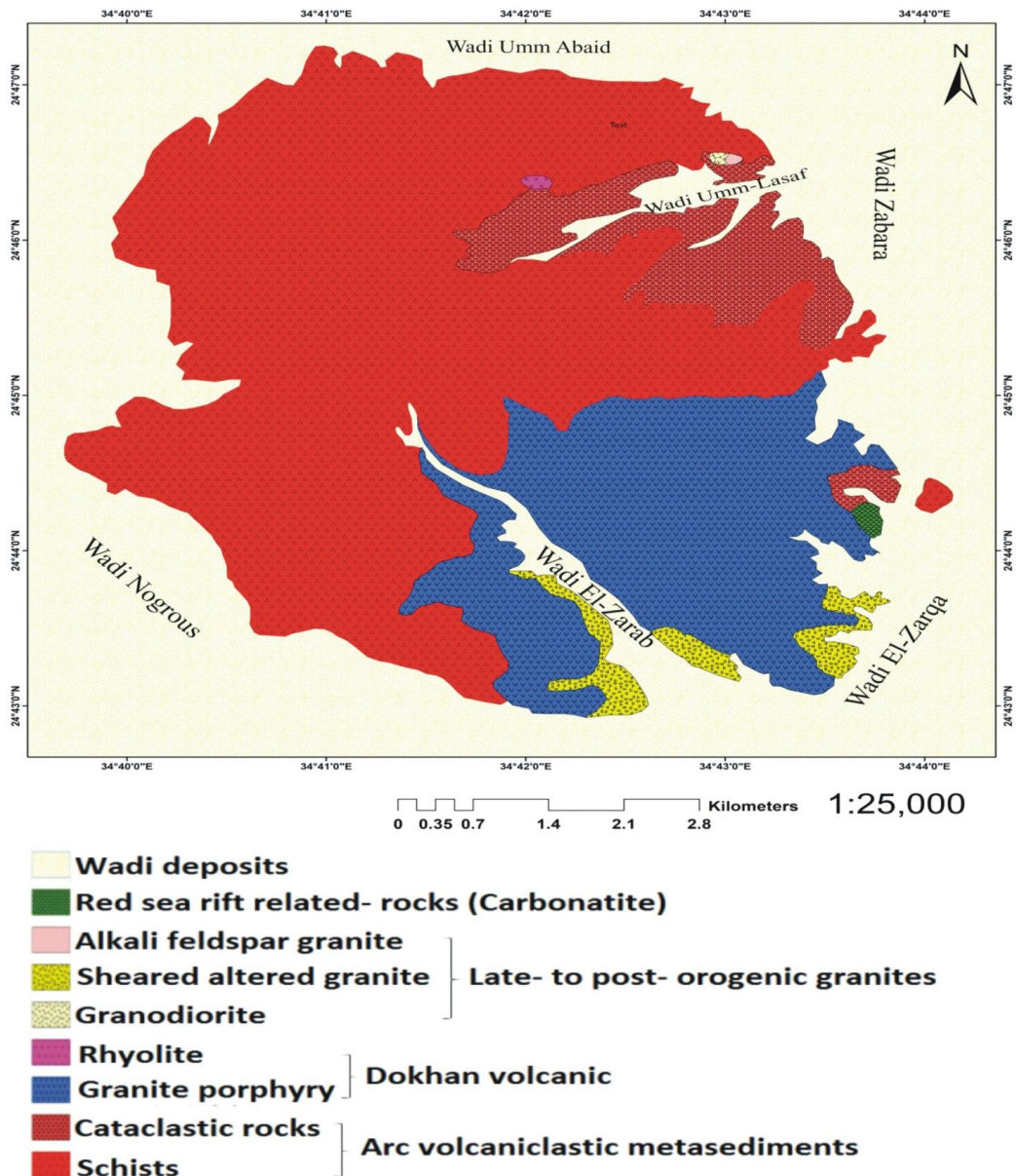


Fig.1. Geological map of Gabal Zabarah, South Eastern Desert, Egypt (Modified after EMRA, 1997).

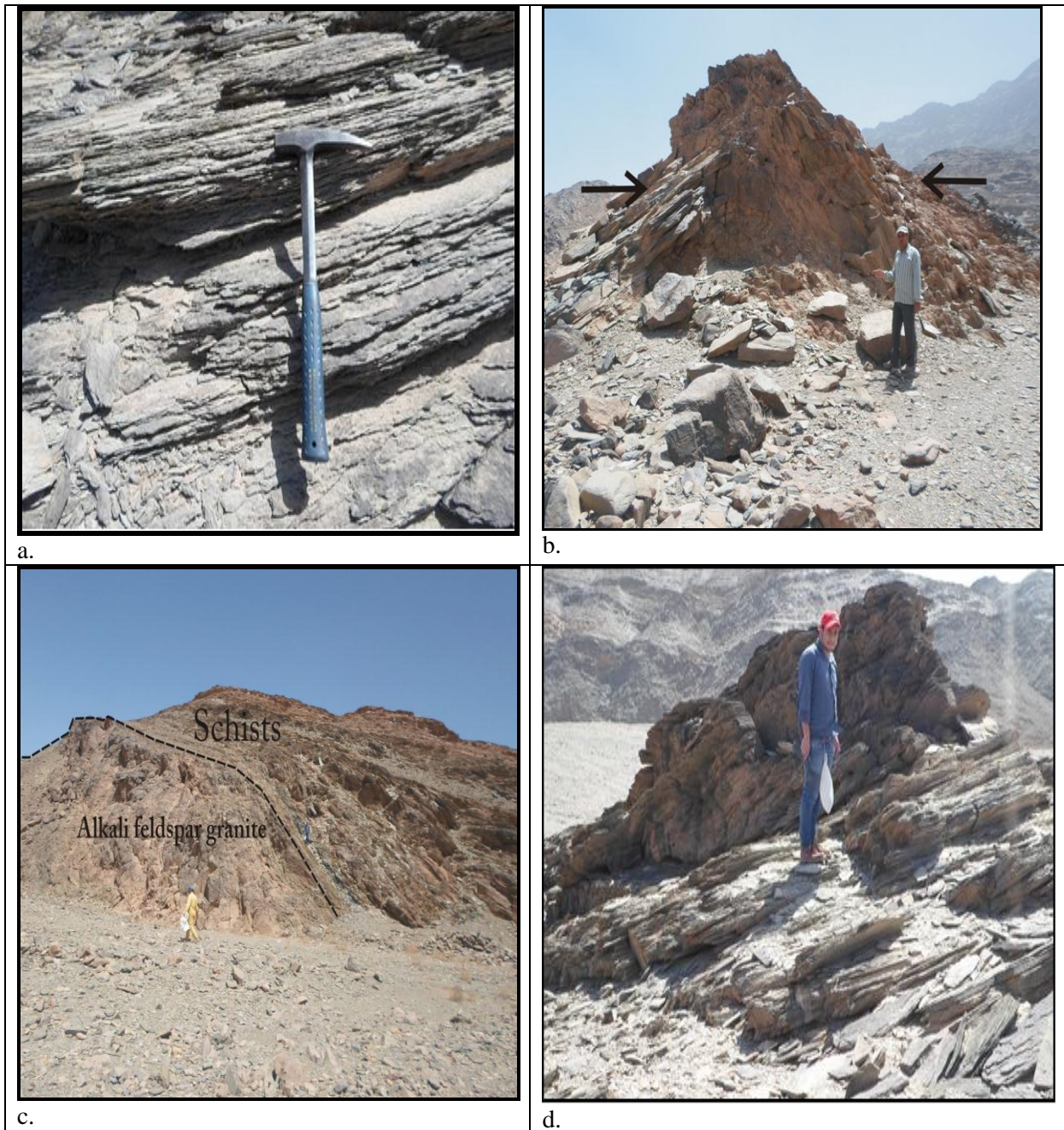


Fig.2(a-d). Field photographs of the outcrops of metasediments showing:

- a. Foliated schists of Wadi Umm Lasaf at Gabal Zabarah (looking at NE).
- b. Anticline folds of schists at Wadi Umm-Lasaf (looking at SE).
- c. The contact between Gabal Zabarah schists and the granitic intrusion (looking at SW).
- d. The cataclastic rocks at Wadi Umm Lasaf (looking at NE).

They can be classified into:-

Tremolite-actinolite schists are fine- to-medium-grained and show wide varieties in color ranging from dark greyish to grey and from pale bluish green to yellowish green. These rocks are highly tectonized, foliated with minor open fold.

Graphite schists are of minor distributions only exposed in the form of bands with average (1.5m) thickness. They are fine-grained, black-green to greyish black in color, highly foliated and mainly composed of graphite.

Tourmaline-bearing schists display patterns of strong metasomatic alteration, with secondary formation of hydrated minerals such tremolite and actinolite, greenish grey to dark grey in color.

Beryl-bearing schists occur at the contact between schists and granitic rocks. There is one of the old mine for emerald in the study area.

Quartzitic schists are characterized by white grey color, hard, coarse-grained and have the same direction of the foliation of the other schists.

Garnet-bearing schists are characterized by rhombic crystals of garnet, they are fine-grained, poorly to well foliated and whitish grey or yellow color.

2. Cataclastic rocks

The cataclastic rocks are widely distributed at Wadi Umm Lasaf in the northern part of the study area (Fig.2d), with less distribution at the southern part. The cataclastic rocks in the study area represented by protomylonitic, blastomylonitic, and ultramylonitic schists.

a. Protomylonitic schists

The protomylonitic schists are coarse to very coarse-grained, green to dark greenish grey in color.

b. Blastomylonitic schists

The blastomylonitic schists are medium grained, grey to greenish grey in color well banded and strongly foliated.

c. Ultramylonitic schists

The ultramylonitic schists are light yellow to brownish yellow in color, fine to medium-grained. The cataclastic rocks show direct contact with the arc volcanoclastic metasediments (Fig.2d). On the other hand, they are directly extruded by rhyolite.

Sampling and Analytical Techniques

17 thin sections were prepared for petrographical investigation of the collected samples (Fig.3). These thin sections were studied under Polarizing Microscope (Optika B-353POL) at the Department of Geology, Faculty of Sciences, Al-Azhar University, Egypt. About 50 photographs were taken in order to investigate textural relations, mineral assemblage, mineral relationships, main textures and microstructures. Chemical analysis of 17 samples from the studied arc volcanoclastic metasediments are carried out to determine major and trace elements. The X-ray fluorescence technique (XRF) is used to determine the trace element concentrations (ppm) via PHILIPS X' Unique-II spectrometer with automatic Sample changer PW 1510. This instrument is connected to a computer system using X-40 program for spectrometry. X-ray diffraction technique (XRD) is used to identify the unknown minerals using PHILIPS PW 3710/31 diffract meter, scintillation counter, Cu-target tube and Ni filter at 40 kV and 30 mA. This instrument is connected to a computer system using powder diffraction program and PDF-2 data base for mineral identification.

RESULTS AND DISCUSSIONS

1. Petrography

The studied metasediments are represented by psammitic and psammopelitic schists and cataclastic rocks are petrographically interpreted as follow:-

I. Psammitic and psammopelitic schists

Psammitic and psammopelitic schists are subdivided into several varieties:-

1. Tremolite-actinolite-zoisite schists
2. Tremolite-tourmaline schists
3. Carbonate schists
4. Fibrolite schists
5. Quartzite schists
6. Pyrophyllite schists

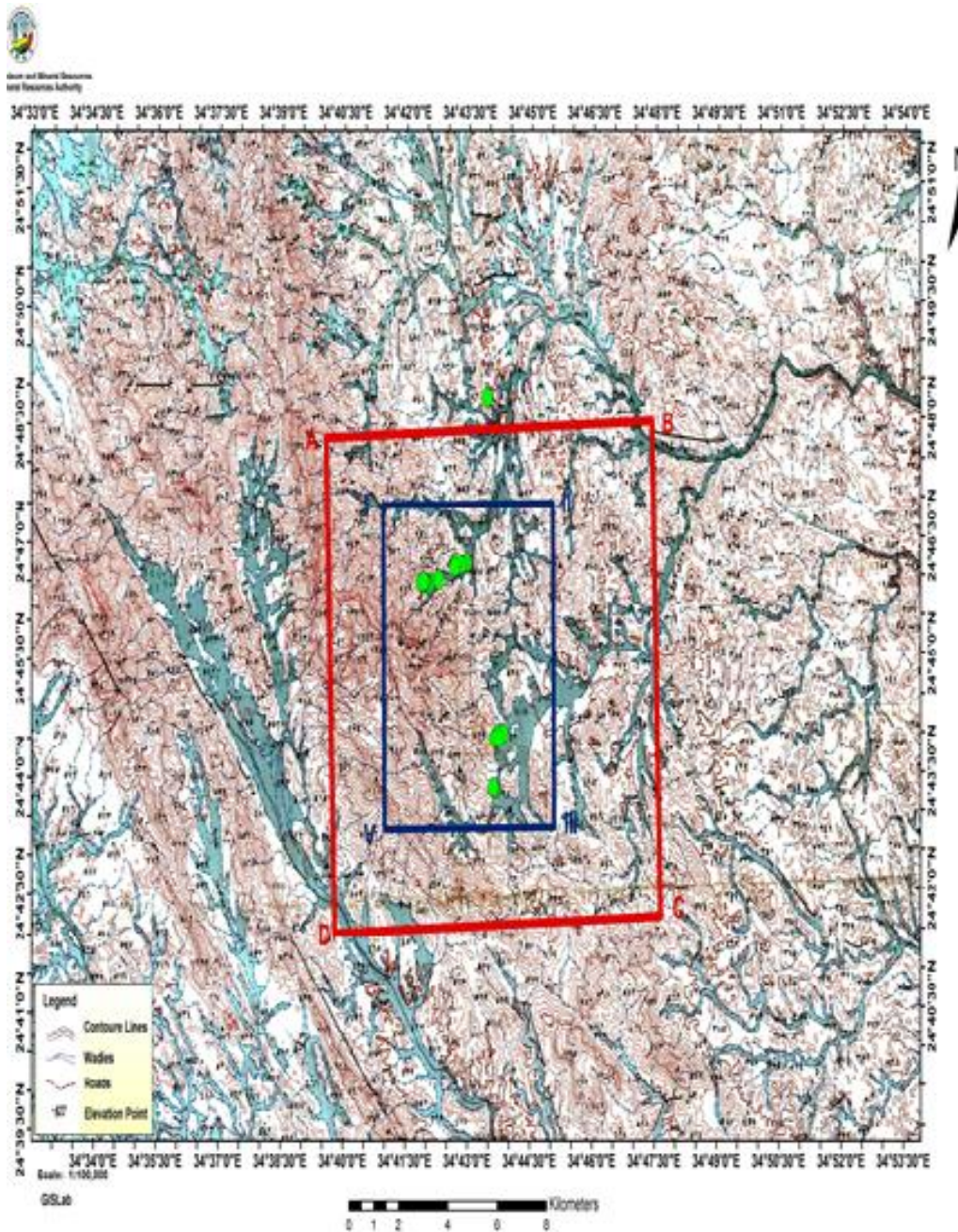


Fig.3. Topographic map showing the distribution of the collected samples.

1. Tremolite-actinolite-zoisite schists are fine- to medium-grained, varying in color from dark greyish to grey and brown, rich in zoisite (up to 50%) and actinolite tremolite. Microscopically, it consists essentially of zoisite, actinolite and tremolite as well as some secondary minerals such as quartz; with opaque minerals as accessory minerals. **Zoisite** occurs as euhedral to subhedral crystals medium- to coarse-grained. It is colorless mineral with high interference color and occurs as granoblastic shape, mostly

exhibits short prismatic crystals, high relief and sharp contact with the surrounding minerals. **Actinolite** is pale green color and exhibits high interference color, usually fibrous in shape and wrapped with tremolite and zoisite (Fig.4a). **Tremolite** is colorless mineral with low interference color and occurs as asbestos form or flaky and fibrous like crystals, fine- to very fine-grained, parallel to the foliation and schistose texture usually associated with actinolite. **Quartz** is also present as secondary mineral, represented by fine- to medium

distributed grains. It occurs as colorless with shadow or wavy extension and characterized in granular shape, filling between the early crystallized minerals. **Opagues** are present as accessory minerals, no more than 1.5% exhibiting anhedral crystals with irregular shape, fine to medium dark grains, most probably of iron oxides.

2. Tremolite-tourmaline schists are medium- to coarse grained, exhibiting vary color from light green to dark green with asbestos form, rich in tourmaline up to 60% and tremolite up to 40%. It is composed essentially of tremolite and tourmaline minerals.

Tourmaline is the main mineral constituent of this rock.. Tourmaline occurs as colorless mineral with high interference color, medium- to coarse-grained, exhibit euhedral to subhedral hexagonal crystals, exhibit two sets of cleavage and sharp contact with the surrounding and wrapped tremolite (Fig.4b). **Tremolite** is colorless mineral with high interference color and occurs as asbestoform or flaky and fibrous - like crystals.

3. Carbonate schists are fine- to medium grained, exhibiting grey, dark grey and brown color. It is rich in carbonate minerals more than (80%). Microscopically, it is composed essentially of calcite, dolomite and magnesite with some secondary minerals such as quartz and opaque minerals.

Calcite is the main mineral constituents of this rock. It exhibits euhedral crystals and sometimes occur as subhedral crystals. It is colorless mineral with high interference color medium- to coarse-grained and occurs as granular, rhombohedral and sometimes large crystals. It is characterized by three sets of cleavage and sharp contact with the surrounding minerals (Fig.4c). **Dolomite** occurs with relatively considerable amount, but less than the calcite. It is colorless mineral with low to medium interference color, fine- to medium-grained, euhedral to subhedral crystals and occurs as rhombohedral shape. **Magnesite** is relatively less in amount exhibits euhedral to subhedral crystals, colorless mineral with high interference color and occurs as plate shapes. **Quartz** is also present as secondary mineral,

fine to medium grains with subhedral crystals. It occurs as colorless minerals with shadow extension and characterized by granular and elongate shape, invading the spaces among the carbonate crystals. **Opagues** are fine to medium grains with irregular shape with dark brown color and associated with the carbonate minerals, filling the fracture of calcite crystals .

4. Fibrolite schists show different colors, graduated from dark grey to dark brown, medium- to coarse-grained, composed essentially of fibrolite up to 60% and quartz up to 30% as well as some secondary minerals such as carbonate and opaque minerals.

Fibrolite is colorless mineral with medium- to coarse-grained, showing euhedral crystals and sometimes exhibiting subhedral crystals with fiber shape (Fig.4d). **Quartz** of the fibrolite schist varies gradually in grain size from very fine to coarse grains, colorless mineral with shadow extension, euhedral to subhedral crystals and usually associated with fibrolite and other minerals. Due to deformation it exhibits polygonal crystal shape with schistos texture. **Carbonate** occurs as secondary mineral is aggregated crystals or veinlets disseminating through other mineral constituents. It occurs usually as colorless minerals with low to medium interference color. **Opagues** are dark brown color, present as irregular shape, usually as iron oxides.

5. Quartzite schists are light grey to dark grey color, fine- to medium-grained, rich in quartz up to 65% and microcline. Microscopically, it consists essentially of quartz, microcline and muscovite with some secondary minerals such as zoisite and biotite, apatite occurs as an accessory mineral.

Quartz is the main mineral constituent represented by fine- to medium-grained, euhedral to subhedral crystals with granular shape. Sometimes, it occurs as veinlets invading the rock mineral constituent with colorless to shadow or wavy extension. **Microcline** presents as essential mineral, but less than quartz. It is colorless with no interference color and exhibits cross-hatching twinning. It is formed as plates and prismatic crystals, fine- to medium-grained with

subhedral crystal. **Muscovite** is medium- to coarse-grained, subhedral crystals with asbestos form shape, colorless mineral and shows high interference color. It exhibits one set of cleavage. **Zoisite** occurs as colorless mineral with high interference color, high relief and as short prismatic crystals. **Biotite** occurs as secondary mineral, but less than zoisite. It is dark brown color with moderately pleochroic from, pale brown to dark brown. It occurs as irregular flakes filling the spaces of early crystallized minerals. **Apatite** exhibits as accessory mineral. It is light greenish yellow in color with moderately pleochroic from dark greenish yellow to honey to dark brown color. It exhibits as small hexagonal crystals with high relief and contain the opaque minerals.

6. Pyrophyllite-tremolite schist has various colors, graduated from yellow to brown color and dark green color, very fine grained, rich in tremolite and pyrophyllite, and composed essentially of tremolite, pyrophyllite and quartz, as well as some secondary minerals such as zoisite.

Tremolite is medium- to coarse-grained, euhedral to subhedral crystal and occurs in most cases as flaky and fibrous like shape, wrapped with the pyrophyllite. It occurs as colorless mineral with high interference colors (Fig.4f). **Pyrophyllite** occurs with relatively considerable amount, but less than tremolite. It is colorless mineral with high interference color, medium- to coarse-grained, euhedral to subhedral crystals and exhibits as asbestos form. Tremolite and pyrophyllite are parallel to the foliation and schistose texture (Fig.4e). **Quartz** is medium- to coarse-grained, euhedral to subhedral crystals with granular and elongate shape. It is colorless minerals with shadow or wavy extension. Quartz invades the spaces between the tremolite and pyrophyllite. **Zoisite** occurs as secondary mineral. It is colorless with high interference color, occurs as medium- to coarse-grained, subhedral crystals with granular and platy shape, high relief and soft contact with the surrounding crystallized minerals.

II. Mylonitic schists

The cataclastic rocks are represented by mylonitic schists. These rocks can be subdivided into several subtypes.

1. Protomylonitic schists

The protomylonitic schists are coarse- to very coarse-grained, green to dark greenish grey in color and represented petrographically by biotite and quartz mylonitic schists.

Biotite-quartz-mylonitic schists are rich in quartz, biotite and plagioclase. Microscopically, it exhibits protomylonitic texture and consists essentially of quartz, biotite and porphyroblasts of plagioclase, with some secondary minerals as sericite, zoisite, epidote associated with accessories of allanite and opaques.

Quartz presents as colorless, fine to medium grains, granular shape and euhedral to subhedral crystals. Due to deformation it occurs as stretched deformed crystals, filling the spaces among the biotite and plagioclase sometimes occurs as a fine groundmass of the biotite-quartz-mylonitic schist. **Biotite** occurs as dark brown color with moderately pleochroic from dark brown to black, fine- to medium-grained and anhedral crystals. Due to deformation it is partially altered to chlorite. It occurs as irregular flakes filling the fracture of the mylonite schists and wrapped with the plagioclase, exhibiting one set of cleavage. **Plagioclase** occurs as coarse- to very coarse-grained porphyroblasts of this rock with euhedral to subhedral crystals. It occurs as colorless, lamellar twinning and sometimes shows zonation, high relief and sharp contact with the surrounding crystallized minerals. Due to deformation it is highly altered to epidote and sericite (Fig.5a). **Sericite** occurs as alteration product of plagioclase crystals, it is colorless with worm-like shape. **Zoisite** occurs as altered plagioclase colorless secondary mineral with high interference color, high relief and occur as short prismatic crystals, sometimes it shows granular shape, euhedral to subhedral crystals. **Epidote** occurs as secondary mineral after plagioclase but relatively less in amount. It is colorless and shows granular to columnar aggregates. **Allanite** is brown color presents as accessories and containing opaques which characterized by dark grains most probably of iron oxides.

2. Blastomylonitic schists

The blastomylonitic schists are medium-grained, well banded and strongly foliated. They are represented petrographically by the following:-

2.1. Quartz-plagioclase mylonitic schists

2.2. Sillimanite-quartz mylonitic schists

2.3. Sericite-perthite-mylonitic schists

2.1. Quartz-plagioclase mylonitic schists are medium-to coarse-grained, yellow to light brown in color, rich in plagioclase, quartz and graphite. Microscopically, it exhibits blastomylonitic texture and consists essentially of porphyroclasts of plagioclase, quartz as well as fine-grained graphite. The secondary minerals are calcite and epidote.

Plagioclase occurs as colorless, large platy crystals, exhibiting porphyroclast of this mylonite schist. Due to deformation it strongly altered to calcite and epidote in a processes known by carbonization and epidotization respectively. **Quartz** occurs with relatively considerable amount, but less than the plagioclase. It is represented by fine- to medium-grained, granular and elongate shape and subhedral crystals. **Graphite** occurs as fine-grained black irregular patches and shows strong orientation parallel to the foliation and filling this mylonite schist. It represents the opaque minerals. **Calcite** presents as colorless secondary mineral with high interference color, medium- to coarse-grained and occurs as granular shape. It is characterized by three sets of cleavages, rhombohedral shape and sometimes as big plates (Fig.5b). **Epidote** occurs as colorless with high interference color and occurs as alteration product of plagioclase and shows a granular to columnar aggregate crystals.

2.2. Sillimanite-quartz mylonitic schists vary in color from grey to dark grey color and light green color, medium- to coarse-grained, rich in quartz, sillimanite and plagioclase. Petrographically, it exhibits blastomylonitic texture and consists essentially of quartz, sillimanite and porphyroclasts of plagioclase with some secondary minerals as epidote.

Quartz varies in grain size from fine, medium to coarse grains, euhedral to subhedral

crystals, granular shape, due to deformation sometimes it exhibits stretched deformed crystals. Quartz shows veinlets invading the spaces between the large plates of plagioclase. **Sillimanite** occurs as colorless with high interference color, fine- to medium-grained, euhedral to subhedral crystals and long prismatic shape. Sillimanite crystals fill the fractures of these mylonite schists (Fig.5c). **Plagioclase** is colorless with relatively considerable amount, but less than the quartz and sillimanite. It is coarse grained with euhedral to subhedral crystals, and altered to epidote. **Epidote** is fine to medium grains, occurs as colorless with high interference color and occurs as alteration product of plagioclase crystals in a process called epidotization. It shows euhedral to subhedral, granular to columnar aggregate crystals.

2.3 sericite-perthite-mylonitic schists are grey to dark grey in color, fine to medium grains, and rich in perthite, plagioclase and quartz. Microscopically, it exhibits blastomylonitic texture and consists essentially of porphyroclasts of perthite, plagioclase, quartz set in fine-grained quartz and microcline. Sericite and epidote occurs as secondary minerals.

Perthite is characterized by intergrowth between plagioclase and K-feldspar (microcline or orthoclase). It is colorless and occurs as euhedral to subhedral platy crystals, coarse grains and associated with plagioclase and microcline as porphyroblasts. It is filled by sericite and epidote as alteration products. **Plagioclase** occurs with relatively considerable amount, but less than the perthite. It occurs as coarse grains, exhibiting large plate crystals and filled by sericite and epidote as alteration products of plagioclase and potash feldspars. **Quartz** is relatively less in amount, represented by medium to coarse distributed grains, shows granular shape and stretched deformed crystals. It is colorless mineral with wavy extension and wrapped with the porphyroclasts of perthite and plagioclase (Fig.5d). **Microcline** presents as colorless

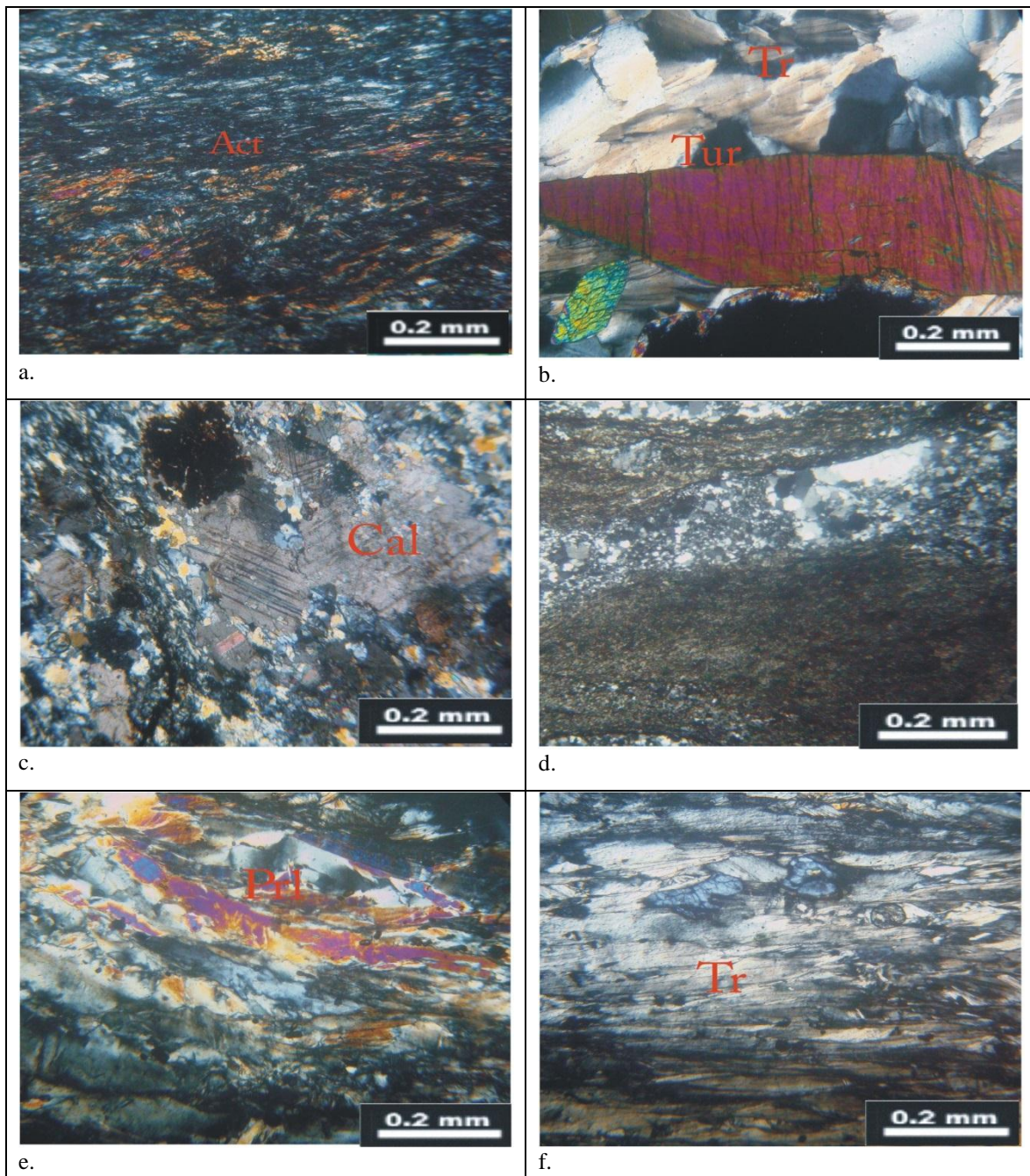


Fig.4 (a-f). Photomicrograph of psammitic and psammopelitic schists (Abbreviations after Kretz, 1983).

- a. Fibrous tremolite-actinolite (Act) crystals (C.N, 25 X).
- b. Large hexagonal of tourmaline (Tur) crystals (C.N, 25 X).
- c. Calcite (Cal) with three sets of cleavage present in the carbonate schist (C.N, 25X).
- d. Fibrolite minerals associated with the quartz crystals (C.N, 25X).
- e. Fibrous pyrophyllite (Pr1) crystals (C.N, 25X).
- f. Asbestoform of tremolite (Tr) and pyrophyllite (C.N, 25X).

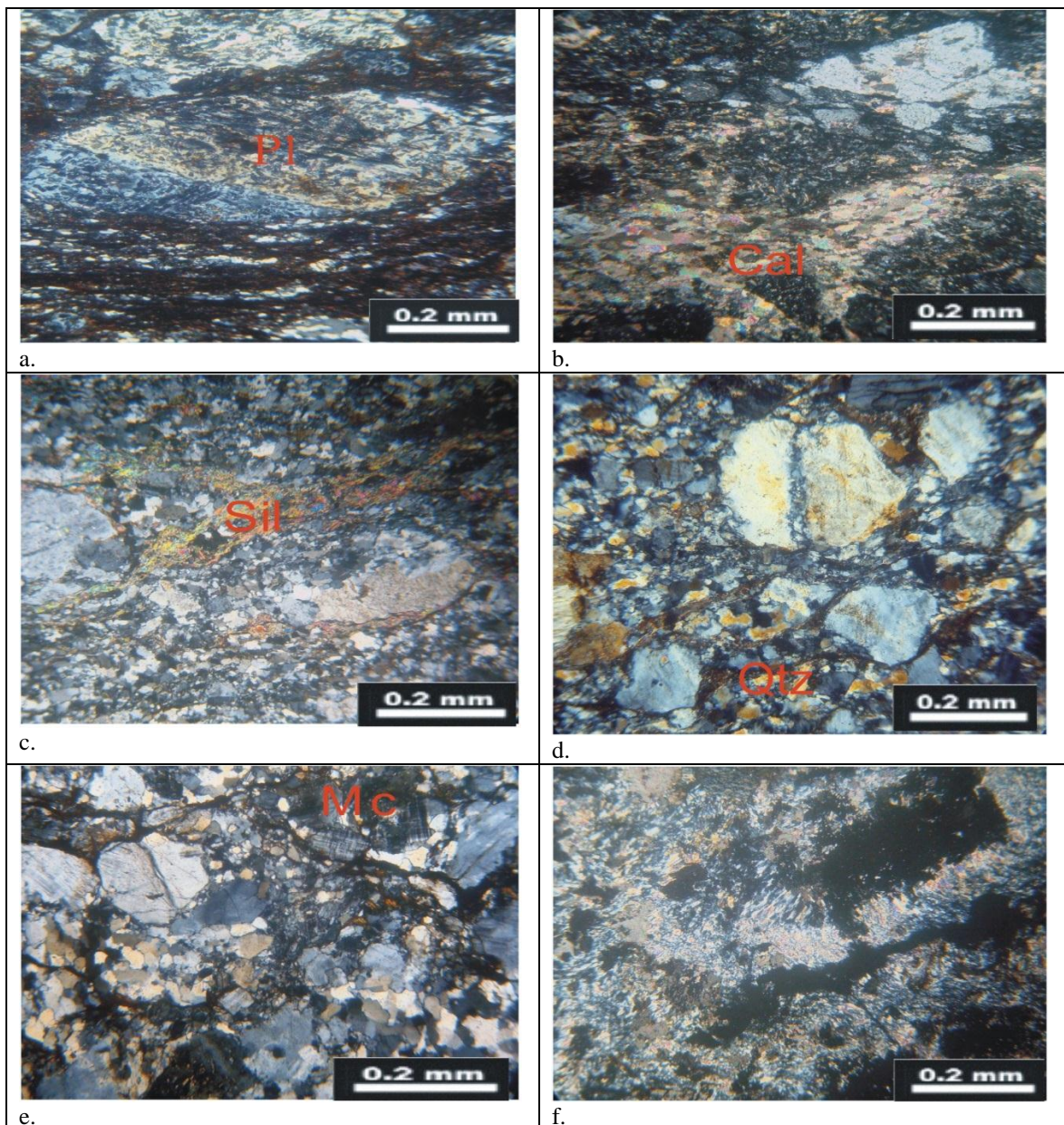


Fig.5 (a-f). Photomicrograph of mylonitic schists.

a. Large plates of plagioclase (Pl) altered to epidote (C.N, 25 X).

b. Calcite associated with graphite, quartz and plagioclase crystals (C.N, 25 X).

c. Fracture filling by the sillimanite (Sil) crystals (C.N, 25X).

d. Fine to coarse-grains of quartz (C.N, 25X).

e. Microcline (Mc) appears as porphyroblasts and associated with quartz (C.N, 25X).

f. Opaque mineral dispersed within the tremolite and calcite (C.N, 25X).

with cross-hatching twinning, euhedral to subhedral plates and prismatic crystals, medium to coarse grains. It occurs as porphyroblasts associated with perthite and plagioclase. **Sericite** occurs as colorless mineral and as worm-like shape crystals, filling the fracture of perthite, plagioclase and invading the spaces among the early crystalized minerals. **Epidote** occurs as alteration product. It is fine to medium grains, colorless mineral and exhibits high interference color.

3. Ultramylonitic schists

The ultramylonitic schists are light yellow to brownish yellow in color, fine- to medium-grained and represented petrographically by the following:-

3.1. Quartzofeldspathic-mylonitic schists

3.2. Tremolite-calcite mylonitic schists

3.1 Quartzofeldspathic-mylonitic schists are yellow to brown color, fine to medium grains and rich in feldspathic minerals such as microcline and orthoclase. Petrographically, it exhibits ultramylonitic texture and consists essentially of porphyroclasts of perthite, microcline and plagioclase with quartz as essentially mineral. The secondary minerals are sericite and zoisite. The opaque minerals are present as accessory minerals.

Perthite is euhedral to subhedral platy crystals, coarse grains and exhibits cluster texture with the surrounding porphyroblasts crystals. **Microcline** occurs as coarse grains, euhedral to subhedral plate crystals. It is colorless and shows cross-hatching twinning, medium relief and presents as porphyroclasts crystals, associated with perthite and plagioclase (Fig.5e). **Plagioclase** occurs as porphyroclasts crystals. It is colorless mineral and shows lamellar twinning, sometimes it exhibits percline twinning. It occurs as large platy crystals and filled by zoisite and sericite in a process called sassuritization and sericitization. **Quartz** shows wide range of grain size, ranging from fine to coarse grains with euhedral to subhedral, granular to elongate crystals. It is colorless mineral and has shadow extension. **Sericite** occurs as colorless mineral, fine to medium grains and exhibits euhedral to

subhedral worm-like crystals, filling plagioclase crystals and invading the spaces among the early crystalized minerals. **Zoisite** occurs as secondary mineral but less than the sericite, it is colorless with interference color, high relief and occurs as short prismatic crystals, sometimes it shows granular shape with euhedral to subhedral crystals.

3.2. Tremolite-calcite mylonitic schists are yellow to brown color, fine to coarse grained and rich in calcite and tremolite. Microscopically, it exhibits ultramylonitic texture and consist essentially of calcite and tremolite with opaques as accessory minerals.

Calcite is colorless with high interference color, euhedral to subhedral granular crystals, medium-to coarse grained and wrapped with tremolite crystals and shows two sets of cleavage. **Tremolite** occurs as euhedral to subhedral asbestiform or flaky and fibrous like crystals, medium- to coarse-grained. It occurs as colorless mineral with high interference color. **Opaque minerals** are characterized by dark colors most probably iron oxides (Fig.5f).

2. Geochemistry

Major oxides composition

The investigated psammitic and psammopelitic schists and cataclastic rocks comprise quartzite schists, garnet schists, pyrophyllite schists, carbonate schists, fibrolite schists, tremolite-actinolite schists and mylonitic schists.

According to data given in tables (1& 3) it is clear that **SiO₂** content shows slightly increasing in the quartzite schists than the other schists. **Al₂O₃** is nearly similar in garnet schist, quartzite schist and tremolite-actinolite schist, but higher than those in pyrophyllite, carbonate and fibrolite schists. **FeO^t** is more enriched in pyrophyllite, fibrolite and tremolite-actinolite schists than quartzite and garnet schists. **MgO** content in pyrophyllite and fibrolite schists is higher enriched, moderate in carbonate and tremolite-actinolite schists and least enriched in quartzite and garnet schists. Carbonate schist is more enriched in **CaO** than other schists. **Na₂O** is high in quartzite and garnet schists. On the

other hand K_2O is high enriched in pyrophyllite schist while very poor in the other analyzed rocks.

Trace Elements Composition

16 trace elements have been detected for the examined psammitic and psammopelitic schists and mylonitic schists. These are V, Cr, Ni, Cu, Zn, Co, Rb, Sr, Y, Zr, Nb, Ba, La, Yb, Ta and Pb (Tables 2 & 4).

There are low variations of Co, Nb, Ta and Pb with high variations of V, Cr, Ni, Cu, Zn, Rb, Sr, Y, Zr, Ba, La and Yb in the psammitic and psammopelitic schists. Meanwhile, the mylonitic schists show low variations of Co, Nb, Ta, Y, La and Pb as well as high variations of V, Cr, Ni, Cu, Zn, Rb, Sr, Zr, Ba and Yb.

Actually it has been observed that V, Cr, Cu, Zn, Co, Rb, Sr, Y and Nb are more enriched in psammitic and psammopelitic schists than mylonitic schists but no great variation in Ni, Zr, Ba, La, Yb, Ta and Pb values. This can be attributed essentially upon the slight variation of their mineralogical composition

The studied rocks are chemically classified the petrochemical characteristics of the psammitic and psammopelitic schists and mylonitic schists are given in several variation diagrams depending on the major oxides. These variation diagrams are used to clarify the nature of the psammitic rock are produced from metamorphism of arenaceous rocks (sandstones) and pelitic rock are produced from metamorphism of argillaceous rocks (shale and clays); a brief discussion to the various binary and ternary diagrams will be given here under.

The studied schists are related to the fields of magnesian hornblende and pelitic schist as shown by using the ACF diagram (Fig.6a) of **Fyfe *et al.* (1958)**. The studied schists fall in shales and carbonates fields according to the $(SiO_2)-(Al_2O_3+Fe_2O_3)-(CaO+MgO)$ ternary diagram (Fig.6b) of **Mason and Moore (1982)**.

On the A'KF ternary diagram of **Winkler (1976)**, the analyzed samples of the study area fall in the fields of biotite and metapelites

(Fig.6c). On the $\log [(Fe_2O_3/K_2O)-(SiO_2/Al_2O_3)]$ of **Pettijohn *et al.* (1972)** and modified by **Herron (1988)**, the plotted samples fall in the fields of greywacke and lithic arenite (Fig.6d).

The following diagrams while, the Al_2O_3 -CaO- (Na_2O+K_2O) diagram (Fig.6e) shows that these schists are of peraluminous and meta-aluminous nature (**Shand, 1951**), i.e. they are rich in alumina.

Al_2O_3 - Na_2O+K_2O diagram (Fig.6f) after **Hermes *et al.* (1978)**, reveals that the examined schists are non peralkaline i.e. poor in alkalines $(Na_2O + K_2O)$.

Tectonic setting

On the $\log FeOt$ - MgO - Al_2O_3 diagram (Fig.7a) of **Pearce and Gale (1977)**, most of the data points fall within field 1 (spreading center island) and field 2 (island arc and active continental margin) fields, it is rich in Al_2O_3 contents.

On the $\log (K_2O/Na_2O)$ versus SiO_2 discrimination diagram of **Roser and Korsch (1986)**, the majority of the points are distributed in the field of passive margin, except two sample, which lies in the island arc field and active continental margin (Fig.7b) due to increase of SiO_2 and K_2O/Na_2O ratio.

Bhatia (1983) used the plots of $(Fe_2O_3^t + MgO)$ versus TiO_2 and Al_2O_3 / SiO_2 ratios in sandstones to discriminate between four types of tectonic settings: A-oceanic island arc (e.g. Marianas and Aleutians), B-continental island arc (e.g. Japan Sea and Cascades), C-active continental margin (Andean type) and D-passive margin. The plotted samples on the diagram (Figs.7c & 7d) fall within or close to fields of continental island arc (B) and passive margin (D) sandstones. The general trend of Gabal Zabarah psammopelitic schist data points indicates a negative correlation between $(Fe_2O_3^t + MgO)$ and (Al_2O_3/SiO_2) . Moreover these ratio values following **Bhatia and Crook (1986)** indicate a continental island arc to passive margin tectonic setting. In this respect **Bhatia (1983)** mentioned that "continental island arcs

or island arcs partly formed on thin continental crust are sedimentary basins adjacent to the oceanic island arcs". This gives an explanation to the sample plotted in the island arc field.

Origin

On the AFM diagram (Fig.7e) of **Hassan**

(1987), the majority of the samples are located in and nearby the metasediments field.

The plotted samples on MgO-Fe₂O₃*-Al₂O₃ ternary diagram after **Nockolds (1947)**, support the metamorphic origin of these rocks (Fig.7f).

Table 1. Major Oxides contents (wt. %) of the psammitic and psammopelitic schists.

Oxides	Quartzite schists			Garnet schists	Pyrophyllite schists				Carbonate schists			Fibrolite schists	Tremolite actinolite schists
	5L	6L	Average	12L	13L	17L	27L	Average	19L	22L	Average	23L	1Z
SiO ₂	73.85	50.12	61.98	65.25	44.33	45.60	43.70	44.54	38.72	42.59	40.65	50.69	48.20
TiO ₂	0.05	0.71	0.38	0.51	0.92	0.21	0.90	0.40	0.63	0.42	0.52	0.48	1.46
Al ₂ O ₃	14.45	13.15	13.8	14.59	14.62	10.61	8.77	11.33	11.85	6.70	9.27	10.57	13.50
Fe ₂ O ₃	1.00	9.93	5.56	6.77	12.84	8.15	12.53	11.17	10.09	6.38	8.23	11.70	10.98
FeO	0.89	8.93	4.91	6.09	11.55	7.33	11.27	10.05	9.07	5.74	7.40	10.52	9.87
MnO	0.04	0.15	0.09	0.09	0.17	0.16	0.2	0.17	0.17	0.31	0.24	0.11	0.17
MgO	0.02	5.95	2.98	1.55	15.02	14.99	15	15	5.93	15.46	10.69	15.06	10.43
CaO	0.31	8.01	4.16	3.16	1.89	7.74	6.29	5.30	13.24	11.99	12.61	2.50	9.28
Na ₂ O	4.19	2.95	3.57	4.23	0.82	1.16	0.10	0.69	0.75	0.10	0.42	0.59	1.90
K ₂ O	3.82	0.66	2.24	0.98	1.22	5.78	7.5	4.83	2.58	0.19	1.38	0.23	0.24
P ₂ O ₅	0.01	0.11	0.06	0.06	0.27	0.02	0	0.09	0.09	0.04	0.06	0.10	0.08
L.O.I	1.77	7.88	4.82	2.53	7.60	5.19	4.74	5.84	15.67	15.52	15.59	7.68	3.53
Total	99.51	99.62		99.72	99.7	99.61	99.73		99.72	99.7		99.71	99.77

Table 2. Trace elements contents (ppm) of the psammitic and psammopelitic schists.

Elements	5L	6L	Average	12L	13L	17L	27L	Average	19L	22L	Average	23L	1Z
V	4.0	238.3	121.15	98.8	197.5	115.3	161	157.93	277	129	203	155	303
Cr	3.2	161.6	82.4	22.2	572.9	1037.2	1225	945.03	250	998	624	1196	414
Ni	4.9	65.4	35.15	12.6	339.4	301.4	716	452.26	84.2	629.3	356.75	541.6	154.2
Cu	2.0	36	19	27.6	18.4	4.9	5	9.43	82.5	34.8	58.65	118.9	43.5
Zn	15.3	78.7	47	27.7	65	224.3	290	193.1	68	62	65	107	80
Co	34.5	37.2	35.85	40.8	41.8	35.4	44	40.4	47.6	32.7	40.15	50.5	45.2
Rb	68.9	48.4	58.65	26.2	24.3	630.3	579.8	411.46	59.8	8.4	34.1	9	7.9
Sr	152.4	210.9	131.65	150.8	221.2	99.2	35.2	118.53	249.4	260.1	254.75	255.4	386.8
Y	18.3	21.1	19.7	17.7	35.7	123.7	105.2	88.2	18.5	16.5	17.5	19.4	25.2
Zr	55.2	59.7	57.45	79.3	158.1	23.4	84.2	88.56	60.4	94.2	77.3	128	114.5
Nb	13.3	11.9	12.6	9.5	13	21.4	30	21.46	11	12	11.5	12.4	12.5
Ba	404.3	127.0	265.65	95	828.6	184.9	293	435.5	213	40	126.5	38	144
La	6.0	2.0	4	2	46.1	2	7.6	18.56	5.8	2	3.9	4.7	5.4
Yb	4.7	17.7	11.2	5.9	94.8	83.4	11	63.06	2	9	5.5	8	2
Ta	2.0	2.0	2	2	2	2	2.1	2.03	2	1.8	1.9	2.2	2
Pb	16.7	5.9	11.3	3.8	8.3	9.9	13	10.4	2	6.8	4.4	7.2	2

Table 3. Major Oxides contents (wt. %) of the mylonitic schists.

Oxides	1L	2L	3L	15L	18L	25L	5Z	Average
SiO ₂	58.90	72.52	53	46.39	70.45	74	37.53	58.97
TiO ₂	1.30	0.17	1.50	0.45	0.26	0.19	0.03	0.55
Al ₂ O ₃	14.48	13.99	16.03	7.95	12.48	13.56	0.57	11.29
Fe ₂ O ₃	9.48	2.09	9.22	8.89	3.10	1.85	5.65	5.75
FeO	8.53	1.88	8.29	7.99	2.78	1.66	5.08	5.17
MnO	0.15	0.03	0.15	0.16	0.06	0.03	0.11	0.09
MgO	4.01	0.33	6.08	24.88	5.00	0.42	30.24	10.13
CaO	3.64	0.56	5.28	2.79	1.23	0.65	2.78	2.41
Na ₂ O	3.76	4.59	3.91	0.39	3.68	4.24	0.01	2.94
K ₂ O	1.39	4.12	1.58	1.89	1.85	3.93	0.01	2.11
P ₂ O ₅	0.27	0.02	0.33	0.02	0.05	0.02	0.01	0.10
L.O.I	2.27	1.28	2.58	5.82	1.51	0.82	22.81	5.29
Total	99.65	99.7	99.66	99.63	99.67	99.71	99.75	

Table 4. Trace elements contents (ppm) of the mylonitic schists.

Elements	1L	2L	3L	15L	18L	25L	5Z	Average
V	97.2	17.4	126.6	125.2	28.0	9.0	34.0	62.48
Cr	26.0	28.0	75.8	959.0	97.2	8.0	2550.0	534.85
Ni	13.8	12.5	48.8	840.5	82.7	5.4	1946.7	421.48
Cu	10.0	4.5	25.7	2.8	3.7	2	8.2	8.12
Zn	97.3	17.2	87.5	116.6	27.5	35.0	38.0	59.87
Co	22.7	2.0	26.7	47.9	27.1	32.8	49.0	29.74
Rb	37.9	51.4	59.6	126.4	35.2	51.7	5.7	52.55
Sr	304.9	78.5	339.4	120.0	263.9	80.3	58.3	177.9
Y	31.2	26.0	38.4	30.2	24.1	28.9	4.0	26.11
Zr	225.9	127.3	196.3	62.0	128.5	100.3	14.3	122.08
Nb	14.6	11.2	15.9	10.1	12.8	12.5	10.6	12.52
Ba	308.5	342.0	336.5	176.9	372.1	239.0	2	253.85
La	12.4	8.3	12.5	4.3	3.5	19.0	2	8.85
Yb	3.5	2.4	14.1	224.3	24.1	0	28.0	42.34
Ta	2.0	2.0	2.0	2.0	2.0	2	2.2	2.02
Pb	10.0	14.3	9.3	6.4	8.8	13.4	3.0	9.31

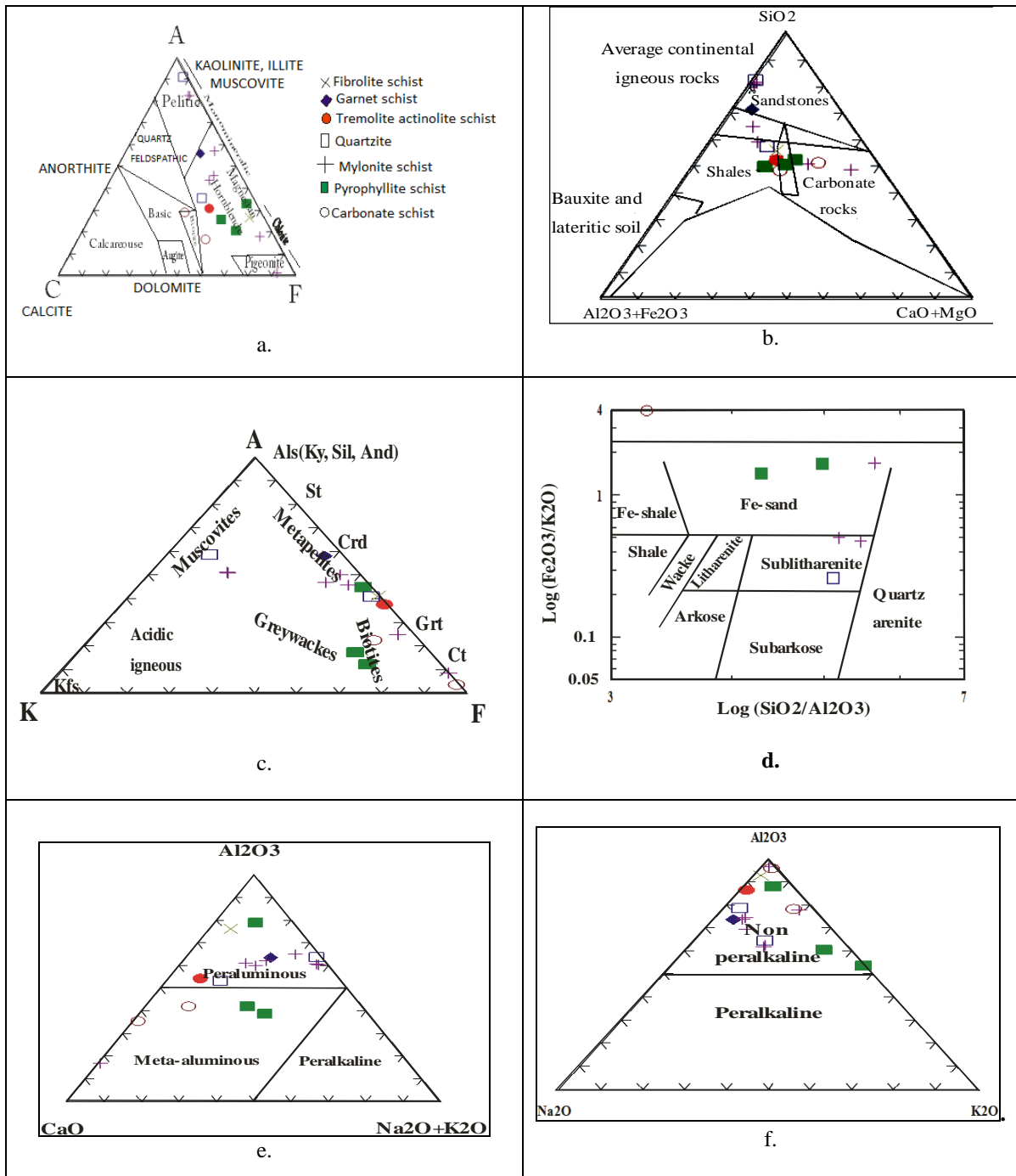


Fig.6. (a-f) Geochemical classification diagrams of the studied metasediments. Symbols as in Fig.(6a).

- a. ACF diagram for the studied metasediments (Fyfe *et al.*, 1958).
- b. (SiO₂)-(Al₂O₃+Fe₂O₃)-(CaO+MgO) diagram for the studied metasediments (Mason and Moore, 1982).
- c. A'KF ternary diagram for the studied metasediments (Winkler, 1976).
- d. (Fe₂O₃/K₂O)-(SiO₂/Al₂O₃) for the studied metasediments (Pettijohn *et al.*, 1972) and modified by (Herron, 1988)
- e. Al₂O₃-CaO-(Na₂O+K₂O) diagram for the studied metasediments (Shand, 1951).
- f. Al₂O₃-Na₂O+K₂O diagram for studied metasediments (Hermes *et al.* 1987)

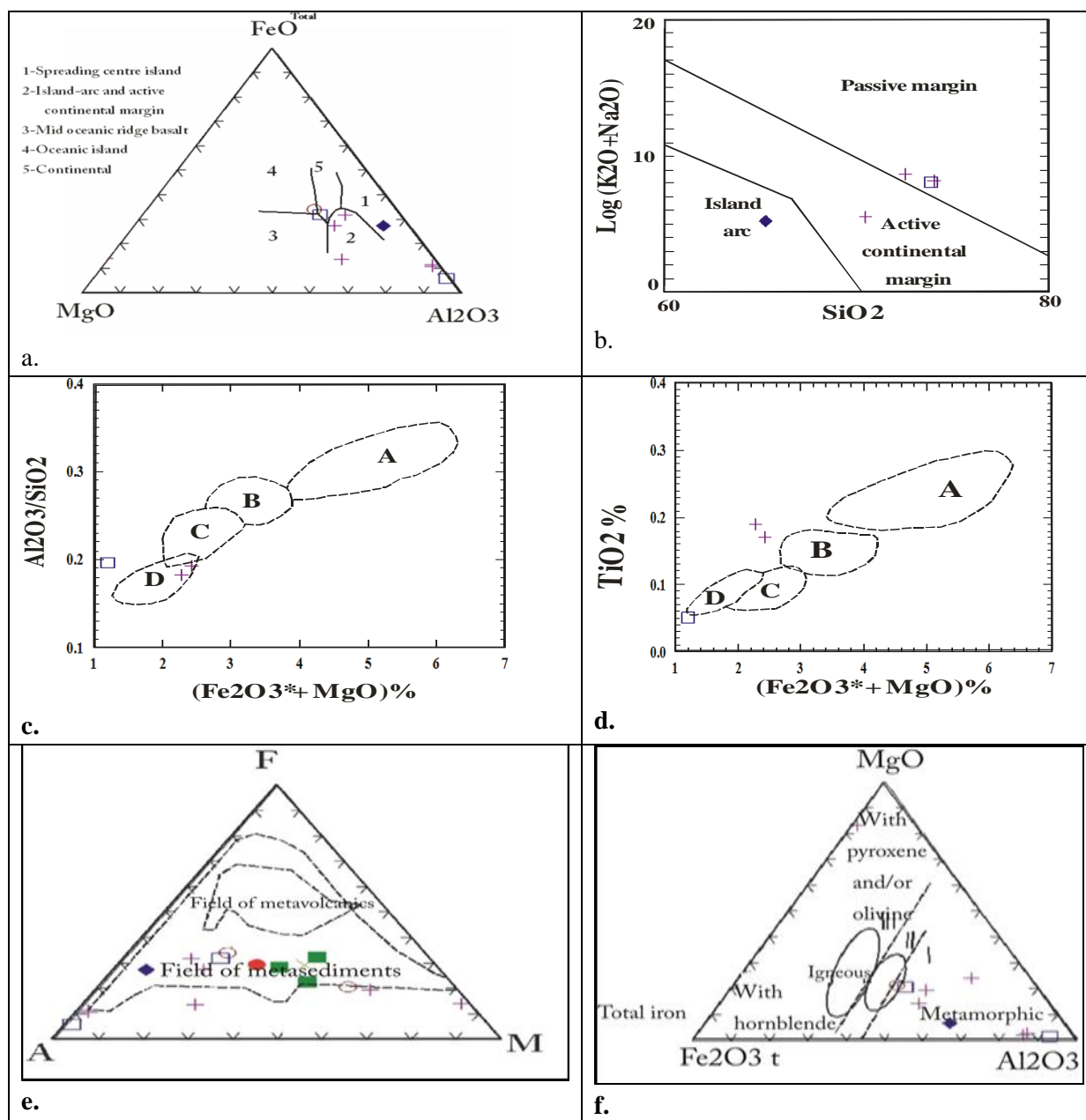


Fig.7. (a-f).Tectonic setting and origin of the studied metasediments. Symbols as in Fig. (6a).

a. FeO^{t} - MgO - Al_2O_3 diagram of the studied schists (Pearce and Gale, 1977).

b. $(\text{K}_2\text{O}/\text{Na}_2\text{O})$ - SiO_2 diagram of the studied metasediments (Roser and Korsch, 1986).

c. $(\text{Fe}_2\text{O}_3^{\text{t}} + \text{MgO})$ - TiO_2 diagram of the studied metasediments (Bhatia, 1983).

d. $(\text{Fe}_2\text{O}_3^{\text{t}} + \text{MgO})$ - $(\text{Al}_2\text{O}_3/\text{SiO}_2)$ diagram of the studied metasediments (Bhatia, 1983).

e. AFM diagram of the studied metasediments (Hassaan, 1987).

f. MgO - $\text{Fe}_2\text{O}_3^{\text{t}}$ - Al_2O_3 diagram of the studied metasediments (Nockolds, 1947).

SUMMARY AND CONCLUSIONS

The present work deals with the geology, petrography and geochemical characteristics of the rock associations of the concerned area. The data and conclusions presented in this work may provide a useful additional mean for identifying, subdividing and grouping the various metasediments whose affinities are not clear in the field and place them in the context of broader geochemical characteristics.

The studied metasediments comprise the psammitic and psammopelitic schists and the cataclastic schists. The psammitic and psammopelitic schists represented by tremolite-actinolite schists, graphite schists, tourmaline-bearing schists, beryl-bearing schists, quartzite schists and garnet-bearing schists. Meanwhile, the cataclastic schists represented by protomylonitic schists, blastomylonitic schists and ultramylonitic schists.

Petrographically, the psammitic and psammopelitic schists comprise tremolite-actinolite-zoisite schists, tremolite-tourmaline schists; carbonate schists, fibrolite schists, quartzite schists and pyrophyllite schists.

Tremolite-actinolite-zoisite schists are composed essentially of tremolite, actinolite, zoisite, quartz and opaques. Tremolite-tourmaline schists composed mainly of tremolite and tourmaline. Carbonate schists composed mainly of calcite, dolomite, magnesite, quartz and opaque minerals. Fibrolite schists composed mainly of quartz, fibrolite, carbonate and opaque minerals. Quartzite schists composed mainly of quartz, muscovite, zoisite, biotite, microcline and apatite. Pyrophyllite schists composed mainly of tremolite, pyrophyllite, quartz and zoisite.

The cataclastic rocks consist of protomylonitic, blastomylonitic and ultramylonitic schists. Protomylonitic rocks are represented by biotite-quartz mylonitic schists. Blastomylonitic schists are represented by quartz-plagioclase mylonitic schists, sillimanite-quartz mylonitic schists and sericite-perthite mylonitic schists. The ultramylonitic schists are represented by quartzofeldspathic

mylonitic schists and tremolite-calcite mylonitic schists.

The biotite-quartz mylonitic schists are composed of plagioclase, biotite, quartz, sericite, zoisite, epidote and allanite. Quartz-plagioclase mylonitic schists composed of plagioclase, quartz, graphite, calcite, sericite and epidote. Sillimanite-quartz mylonitic schists composed of sillimanite, quartz, plagioclase, sericite, epidote and opaque minerals. Sericite-perthite mylonitic schists composed of perthite, plagioclase, quartz, sericite, microcline and epidote. Quartzofeldspathic mylonitic schists composed of plagioclase, perthite, quartz, microcline, biotite, sericite, epidote and opaque minerals. Tremolite-calcite mylonitic schists composed of tremolite, calcite and opaque minerals.

The geochemical characteristics and trace element contents of the metasediments are comparable with those of the continental and oceanic island arc sandstones of **Bhatia (1983)**, which were probably derived from the non-peralkaline, peraluminous and/or metamorphic rocks.

REFERENCES

- Bhatia, M.K., Crook, K.A., 1986.** Trace element characteristics of grey wackes and tectonic setting discrimination of sedimentary basins. *Contrib. Mineral. Petrol.*, 92, 181-193.
- Bhatia, M.R., 1983.** Plate tectonics and geochemical composition of sandstones. *J. Geol.* 91, pp. 611-627.
- EGSMA, 1992.** Hamata Quadrangle Map, Scale 1:250000. Egyptian Geological Survey, Cairo, Egypt.
- Fyfe, W.S., Turner, F.J., Verhoogen, J., 1958.** Metamorphic reactions and metamorphic facies. *Geol. Soc. Am. Memoir* 73.
- Grundmann, G., Morteani, G., 1993.** Emerald formation during regional metamorphism: The Zabara, Sikait and Umm Kabu deposits (Eastern Desert, Egypt). In: Thorweihe & Schandelmeeir (Editors), *Geoscientific Research in Northeast Africa*, Balkema-Rotterdam, pp. 495-498.
- Hakki, W., Hab-Errumman, S., 1996.** Mineralization associated with tectonically emplaced shield edges and related trends in

- North Africa and the Arabian shield. Geol. Surv Centennial Conf. (1896-1996), Egypt. **75**: 303-330.
- Hassaan, M.M., 1987.** Abundance distribution of major elements and their implications on magma type and tectonic setting in the main Proterozoic rock units, Eastern Desert, Egypt. Symposium of Precambrian Geochemistry. Abstract of Lund, Sweden.
- Hermes, O.D., Ballard, R.D., Banks, P.O., 1978.** Upper Ordovician Peralkaline granites from the Gulf of Maine. Geol. Soc. Am. Bull, 80, 1761-1774.
- Herron, M.M., 1988.** Geochemical classification of terrigenous sands and shales from core or log data. J. Sed. Petrol., 58, 820-829p.
- Kretz, R., 1983.** Symbols for rock-forming minerals. Am. Mineral. V. 68, 277-279p.
- Mason, B., Moore, C.B., 1982.** Principles of geochemistry, John Wiley, New York.
- Nockolds, S.R., 1947.** The relation between chemical composition and paragenesis in the biotites of micas of igneous rocks. Amer.J.Sci. V. 245, No. 5, p. 401-420.
- Pearce, J.A., Gale, G.H., 1977.** Identification of ore-deposition environment from trace element geochemistry of associated igneous host rocks. In: Volcanic Processes in ore Genesis. Inst. Min. and Metallurgy, Geol. Soc. London, Spec. Publ. 7, 14-24.
- Pettijohn, F.J., Potter P.E., Siever R., 1972.** Sand and sandstones. Springer-Verlage, New York.
- Roser B.P., Korsch R.G., 1986.** Determination of tectonic setting of sandstone-mudstone suites using SiO₂ content and K₂O/Na₂O ratio. Geol., 94, 635-650.
- Shand, S.J., 1951.** "The Eruptive Rocks" John Wiley, New York.
- Soliman, M.M., 1986.** Ancient mines and beryllium mineralization associated with Precambrian stanniferous granites in the Nugrus-Zabara area, southeastern Desert, Egypt. Arab Gulf J. Sci. Res., V. 4, pp. 529-548.
- Surour, A.A., 1995.** Medium- to high-pressure garnet-amphibolites from Gabal Zabara and Wadi Sikait, south Eastern Desert, Egypt. J. Afr. Earth. Sci. V.21. pp. 443-457.
- Surour, A.A., Takla, M.A., Omar, S.A., 2002.** EPR spectra and age determination of beryl from the Eastern Desert of Egypt. Annals Geol. Surv. Egypt. V. 24. pp. 389-400.
- Takla, M.A., Surour, A.A., Omar, S.M., 2004.** Mapping Source of beryllium and genesis of some beryl occurrences in the Eastern Desert of Egypt. Annals Geol. Surv.. Egypt. V.26. pp. 153-182.
- Winkler, H.G.F., 1976.** Petrogenesis of metamorphic rocks. 4th, edition. Springer-Verlage. Berlin-Heidelberg-New York, 342p.